Title

Localized measures of callosal atrophy are associated with late-life hypertension: AGES-Reykjavik Study.

Journal

NeuroImage, In press

ISSN

1053-8119

Authors

Harris, Peter
Alcantara, Dan A
Amenta, Nina
et al.

Publication Date

2008-07-18

Peer reviewed

Localized Measures of Callosal Atrophy Are Associated with Late-Life Hypertension: AGES-Reykjavik Study[1]

Peter Harris (1), Dan A. Alcantara (2), Nina Amenta (2), Oscar L. Lopez (3), Guðný Eiríksdóttir (4), Sigurður Sigurðsson (4), Villmundur Gudnason (4), Sarah Madsen (5), Paul M. Thompson (5), Lenore J. Launer (6), Owen T. Carmichael (1,2)

1. Department of Neurology, University of California, Davis, CA, USA
2. Department of Computer Science, University of California, Davis, CA, USA
3. Department of Neurology, University of Pittsburgh, PA, USA
4. Icelandic Heart Association Research Institute, Hjartavernd, Iceland
5. Department of Neurology, University of California, Los Angeles, CA, USA
6. Neuroepidemiology Section, National Institute on Aging, Bethesda, MD, USA

[1] Corresponding author:
Owen Carmichael
Phone: 530-754-9657
Fax: 530-754-5136
Email: ocarmichael@ucdavis.edu

Abstract

Hypertension is highly prevalent in elderly individuals and may be associated with cognitive decline, but the mechanisms by which hypertension may impact brain structure, and thereby modulate the time course of late-life cognitive performance, are not well understood. Therefore we used Localized Components Analysis, a novel computational method, to measure spatially-localized patterns of corpus callosum (CC) atrophy in 28 right-handed female subjects aged 75-79 years in the Age, Gene/Environment Susceptibility–Reykjavik Study (AGES–Reykjavik), a large-scale epidemiological study of aging. Localized callosal atrophy in the posterior midbody and splenium was significantly associated with systolic blood pressure in linear statistical models that controlled for age, while associations between blood pressure and anterior CC atrophy measures were not statistically significant. Additionally, overall measures of global CC atrophy were not significantly associated with blood pressure. The posterior CC may be differentially vulnerable to hypertension-associated atrophy, possibly due to its relatively tenuous vascularization.

Introduction

Hypertension increases risks for heart failure, renal failure, and cerebrovascular dysfunction and affects 25% of the adult population in industrialized societies (Lifton et al., 2001, Burt et al., 1995). Hypertension is especially prevalent in the elderly and is associated with risk of late-life cognitive decline (Ong et al., 2007; Launer et al., 1995; Skoog et al., 1996; Kilander et al., 1998; Harrington et al., 2000). Additionally, vascular risk factors such as hypertension may influence how dementias of various etiologies are

expressed clinically (Skoog and Gustafson, 2002; DeCarli, 2004). Due to the high prevalence of hypertension and its possible effects on cognition, an understanding of the biological mechanisms by which chronic hypertension may modulate late-life cognitive decline could have a dramatic public health impact. However, these mechanisms are not fully understood.

This goal of this study is to assess the viability of novel neuroimaging-based measures of brain structure for elucidation of relationships between late-life blood pressure and cognition. Specifically, we use structural magnetic resonance imaging (MRI) scans to measure localized atrophy patterns in the corpus callosum (CC) and relate CC atrophy patterns to blood pressure in 28 nondemented elderly members of a population-based cohort. The CC is an especially important determinant of late-life cognitive function because it is the major white matter tract that connects homotopic cortical regions in the two hemispheres; thus, regional atrophy within the CC can serve as an indirect cue about the integrity of interhemispheric cortical-cortical connections (Thompson et al., 2001, Janowsky et al., 1996). Because specific CC sub-regions subsume specific cortical-cortical connections, localized damage to specific sub-regions may be associated with specific cognitive deficits, motivating the investigation of spatially-localized CC deficits and their differential effects on cognition (Funnell et al., 2000).

Relationships between hypertension and acute brain injury (in the form of MRI-appearing infarcts or hyperintense white matter) have been reported, as have relationships between hypertension and other brain regions, including the ventricles and hippocampus (Chrysikopoulos et al., 1997; Kasow et al., 2000; Yamamoto et al., 2005; Salerno et al., 1992; Korf et al. 2004). However, to the best of our knowledge, specific hypertension-related atrophic changes in the CC have not yet been reported.

Additionally, most prior studies relating brain regional characteristics to blood pressure summarized regional atrophy in terms of overall structure volume or surface area, and thus were unable to measure spatially-localized deficits to CC sub-regions. Finally, most prior studies of the brain structural correlates of hypertension were drawn from clinic-recruited subject cohorts, leading to concerns about the generalizability of results to the elderly population at large.

Here we overcame these limitations using a novel computational method to analyze spatially-localized regional atrophy in a population-based cohort. First, we validated the atrophy analysis method, Localized Components Analysis (LoCA), by using it to detect HIV-associated CC deficits in a 51-subject middle-aged cohort and comparing results to an established spatial mapping method (Alcantara et al 2007; Thompson et al. 2006). Then we used the method to describe spatial patterns of CC atrophy in a sample of 28 subjects from an Icelandic population-based study, and related CC atrophy to blood pressure. The results suggest that LoCA can summarize localized CC atrophy differences that agree with much higher-dimensional approaches, and that LoCA can detect hypertension-related CC deficits that agree with what is known about CC vasculature.

Materials and Methods

Subjects

The Age, Gene/Environment Susceptibility–Reykjavik Study (AGES–Reykjavik) was initiated in 2002 to examine genetic susceptibility, gene/environment interaction, and other risk factors in relation to disease and disability in the elderly (Harris et al. 2007). Subjects were recruited for the AGES–Reykjavik cohort from an established

population-based cohort, the Reykjavik Study, which has been followed since 1967 by the Icelandic Heart Association. AGES–Reykjavik subjects received a comprehensive clinical evaluation, including a cognitive test battery and structural MRI of the brain. From the first 2300 AGES-Reykjavik subjects, we selected those who had completed an MRI scan and clinical evaluation and were right-handed, female, aged 75-79, cognitively normal (MMSE>=26 and no clinical evaluation of mild cognitive impairment or dementia), and without evidence of clinical depression at the time of their clinical evaluation and MRI scan. These criteria were applied to minimize confounding effects of other literature-reported sources of CC variability—including gender, chronological age, and handedness-- on relationships between blood pressure and CC morphology (Weis et al 1993, Parashos et al 1995, Salat et al 1997, Allen et al. 1991). Dementia case ascertainment is a three-step process. The Mini-Mental State Examination and the Digit Symbol Substitution Test are administered to all participants. Persons who are screen positive based on a combination of these tests are administered a second, more diagnostic test battery, and a subset of them are selected for a neurologic examination. Proxies for this latter group are interviewed about medical history and social, cognitive, and daily functioning relevant to the diagnosis. A consensus diagnosis based on international guidelines is made by a panel that includes a geriatrician, neurologist, neuropsychologist, and neuroradiologist. Screening for depression is done at the first clinic visit, with followup testing for screen positives with the Mini-International Neuropsychiatric Interview, which gives more detailed diagnostic information about psychiatric morbidity.

A total of 13 subjects met the above criteria along with all of the following criteria

for hypertension: they indicated in a health history questionnaire that a clinician told them they had hypertension, they were prescribed anti-hypertensive medication which they were currently taking at the time of the clinical evaluation, and they had elevated systolic (>=140 mm/Hg) or diastolic (>= 90 mm/Hg) blood pressure at the time of the clinical evaluation. In contrast, 15 subjects met the following criteria for normal blood pressure: a clinician had never told them they were hypertensive, they had no history of taking anti-hypertensive medication, and they had normal systolic (<120 mm/Hg) and diastolic (<80 mm/Hg) blood pressure at the time of the clinical evaluation. Subject characteristics are summarized in Table 1. As expected, systolic and diastolic blood pressure varied significantly between subjects who did and did not meet the hypertension criteria; differences in other clinical variables were not significant between the groups. Relationships between CC morphology and blood pressure were analyzed in these 28 subjects.

Imaging

All subjects received MRI scans on the same GE Signa Twinspeed Excite 1.5 T MR scanner at the Icelandic Heart Association (IHA) Research Center. Scan sequences included an axial T1-weighted 3D SPGR, an axial proton density/T2-weighted double spin echo sequence, and an axial FLAIR. The T1-weighted three dimensional spoiled gradient echo (3D-SPGR) sequence had the following acquisition parameters: (TE, 8 ms; TR, 21 ms; FA, 30; FOV 240 mm; matrix 256 x 256, slice thickness 1.5 mm). All images were acquired to give full brain coverage and slices were angled parallel to the anterior commissure - posterior commissure line. The IHA uses highly stringent and reproducible daily QA tests based on GE's System Performance Test (SPT) including

signal-to-noise ratio (SNR), radiofrequency (RF) power, geometric distortion, and z-isocenter. In addition, the IHA performs weekly shim and phased-array head coil geometric distortion and SNR tests using the ADNI phantom (Gunter et al, 2007). Monthly EPI, full system/PM testing, and American College of Radiology phantom testing including center frequency, table position, SNR, CNR, geometric distortion, contrast resolution, image uniformity, ghosting, and slice thickness accuracy, and image evaluation were performed.

Corpus callosum tracing and tracer cross-validation

CC were traced on sagittal views of the T1-weighted images of each subject CC by a single rater (P.H.) whose tracings were validated against those of an expert rater on a separate set of validation images. The CC tracing protocol has been described previously (Thompson et al., 2006). Briefly, the rater began by using the AFNI software package to identify the positions of the anterior commissure (AC), posterior commissure (PC), and other anatomical landmarks on each subject's image; the software used these landmarks to affinely re-align the image into a standard position including a midsagittal plane oriented along the cardinal axes of the image and the AC-PC line horizontal. Because this alignment re-scaled the images to place the AC and PC in standard positions, the alignment removed gross inter-subject differences in overall head size from the data, thus helping to insure that gross overall head size did not confound hypertension-related CC effects. The CC boundary was traced in the midsagittal section using the MultiTracer software package (Woods, 2001); these midsagittal tracings were analyzed below to detect localized deficits related to hypertension. However, the tracer additionally traced the CC boundary on a total of 8 additional sagittal slices, 4 on either side of the

midsagittal slice, for a total of 9 slices traced per CC. The rater was blinded to all clinical variables, including age and hypertension status, at the time the tracings were performed.

The 8 additional slices were traced to assess inter-rater reliability between the current rater and previous manual raters on a distinct set of 9-slice CC tracings of middle-aged HIV/AIDS and control subjects from a previous study (Thompson et al 2006). Briefly, our rater traced the CC on 17 scans randomly selected from the prior study cohort of 51 subjects; these included healthy subjects in their 40s as well as those whose CCs were severely atrophied due to HIV/AIDS. The one-way "agreement" type intraclass correlation coefficient in 9-slice callosal volumes between our rater and the previous rater was assessed using the `icc` routine in R version 2.3.1.

Callosal shape analysis

Localized Components Analysis (LoCA) is a technique for automatically describing brain region shape in terms of a small set of morphometric measurements, each of which addresses a distinct surface sub-region (Alcantara et al 2007). Briefly, LoCA takes as input a set of brain region tracings and uses a numerical optimization technique to output a concise set of *shape components*– a set of local deformations of a prototype surface that, together, span the shape variability present in the set of input tracings. The shape components allow particular instances of the brain region to be numerically described in terms of an average prototype region that has had a set of spatially-localized deformations applied to it. In other words, each brain region instance is described in terms of *shape component coefficients*– coefficients that represent the degree to which a particular shape component deformation was applied to the prototype

surface to make it resemble the given region instance. LoCA is similar to principal components analysis (PCA) and independent components analysis (ICA) in that it is a linear subspace method; subject brain regions are expressed as linear combinations of shape components. However, we previously showed that the linear shape components provided by LoCA may provide a more intuitive understanding of the anatomical meaning of individual shape components than competing linear subspace methods (Alcantara et al 2007).

The specific steps performed by LoCA on the 2D midsagital slice of the AGES-Reykjavik CCs were as follows. First, each CC surface was approximated by a set of 200 surface points; the surface points were positioned so that corresponding surface points resided in corresponding anatomical locations across subjects (Ghosh et al., 2007). Each subject's CC surface point set was then translated, rotated, and globally scaled through a Generalized Procrustes Alignment (GPA) to remove intersubject differences in gross geometric characteristics. For each CC, the surface point coordinates were then stacked into a vector, and a linear subspace that spanned the point coordinate vectors across all subjects was estimated. The basis vectors of the linear subspace are the shape components described above; the loadings of each basis vector represent the deformation of a mean CC surface that represents a dominant mode of variability in the population. The unique property of the LoCA method is that the basis vectors are simultaneously constrained to be orthogonal as well as spatially-localized; the spatial locality makes it easier to interpret each shape component as representing atrophy to a specific anatomical sub-region of the CC.

Cross-validation of LoCA with radial thickness mapping

We validated LoCA for CC atrophy analysis by using it to detect localized CC shape differences between middle-aged HIV/AIDS subjects and age-matched controls, and comparing the LoCA results with previously-published results on the same data set from an established, high-dimensional CC atrophy analysis method. The subject pool is the same set of 51 middle aged AIDS and control subjects from which the inter-rater reliability scans were drawn; their clinical characteristics and imaging procedures have been described previously (Thompson et al., 2006). LoCA was used to estimate shape components from the set of 51 CCs; the LoCA shape components that account for the highest degree of intersubject CC variability were presented previously and were compared to those estimated by several competing linear subspace methods (Alcantara et al 2007). For this validation experiment, we selected the 15% of shape components that explain the largest amounts of intersubject CC variability and assessed differences in CC shape between control and AIDS groups by conducting T tests on the LoCA shape component coefficients between groups. We then visualized shape components whose coefficients differed significantly between AIDS and controls, and compared the inter-group shape differences indicated by those shape components to the inter-group shape differences that were indicated by the high-dimensional thickness mapping method and published previously (Thompson et al., 2006).

Statistical analysis

LoCA shape components estimated from the AGES-Reykjavik CCs were visualized and sorted in decreasing order of the percentage of intersubject shape variability they accounted for. Shape components accounting for 5% or more of CC shape variability

were analyzed further to assess associations between patterns of CC atrophy and hypertension. Pre-selecting shape components in this way helped to remove spurious shape components that model random noise patterns in the CC shape data and do not represent true spatial patterns of callosal atrophy. For each selected shape component, visual summary plots of the shape component coefficients were used to assess whether they were normally distributed; coefficients with skewed distributions were log-transformed to encourage normality. All distributions of shape component coefficients appeared reasonably normal after transformation. Then, the shape component coefficients were re-scaled so that a unit change in the coefficient corresponded to a 1-mm change in the position of the CC surface at the surface point that is moved maximally by the shape component. Finally, the signs of the shape component coefficients were flipped, where necessary, so that a positive change in any coefficient corresponded to a contraction in localized CC thickness, and a negative change corresponded to a localized expansion. These coefficient transformations allow easier physical interpretation of the coefficients and regression parameters in the statistical analyses; a shape component coefficient of 1 represents a 1-mm shrinkage in callosal thickness at the CC sub-region indicated by the shape component, and a regression parameter of 1 indicated that a 1-mm drop in localized CC thickness corresponded to a 1-unit increase in blood pressure. These modifications of the shape component coefficients were simple re-scalings that should not affect their underlying relationships with blood pressure.

The relationships between shape component coefficients and systolic and diastolic blood pressure was assessed in linear regression models that controlled for age. F tests were used to assess the significance of coefficient-blood pressure relationships, and the shape components and regression coefficients were used to assess the directionality of

the relationship and what portion of the CC was implicated. Similar linear regression models evaluated the relationship between gross volumetric CC measures and systolic and diastolic blood pressure, controlling for age; overall CC volume from the 9-slice tracing and the magnitude of the scaling parameter from GPA alignment were the gross measures used as outcome variables in these models. We compared regression results between the shape component coefficients and gross volumetric measures to qualitatively assess the value added by the shape components over more traditional CC atrophy measures.

Radial thickness maps similar to those described above were produced to cross-validate the associations between callosal atrophy and systolic blood pressure detected by LoCA. Briefly, local callosal thickness was measured at each point along each subject CC. Correspondences were established at homologous anatomical surface points across CCs and, and at each surface position the local thickness values were correlated with systolic blood pressure. To mirror the LoCA analysis, we adjusted the blood pressure measures for age by fitting a line to a plot of blood pressure against age and replacing the original blood pressure values with the residual of the line fit. The correlations resulted in a correlation coefficient, ρ, at each surface point, and statistical tests were run to assign a *p* value to the hypothesis that $\rho<0$, indicating an association between increasing CC atrophy and increasing blood pressure. The *p* values were rendered in color across the surface to show which sections of the CC had associations between atrophy and blood pressure. We qualitatively compared this spatial map to the LoCA shape components suggesting significant associations between atrophy and blood pressure, to attempt to assess to convergence of the two methods.

Results

Validation

The one-way "agreement" type intraclass correlation coefficient in callosal volumes between our rater and the previous rater on the 17 AIDS and control CCs was .94. Of the 8 shape components accounting for the highest degrees of CC shape variability in the AIDS and control subjects, the ones whose coefficients differed significantly between AIDS and controls are shown in Figure 1. The spatial map indicating CC surface positions for which localized CC radial thickness at that point differed significantly between AIDS and control, previously published, is also shown for reference (Thompson et al 2006). Both methods strongly indicate that atrophy in the genu and some of the more anterior sections of the midbody. Importantly, the shape components indicate that there are at least two sections of the CC surface (in the superior midbody, shown in component E and the genu, shown in component H—whose thickness varies significantly throughout the data set but do not differ systematically between groups. The shape components and spatial map agree on the lack of significant differences in the CC sub-regions indicated by these shape components as well as those indicated by components C, D, and G. We note, however, that there are minor discrepancies between the two methods: the superior-anterior CC midbody reflects a localized deficit in the spatial map but not in the shape components, and genu effects are considered more widespread in LoCA than in the spatial map.

Shape components

The percentage of intersubject shape variability explained by each AGES-Reykjavik shape component was computed. A plot of the percentage of shape variability accounted for by the shape components, listed in decreasing order, is shown in Figure 2. Seven shape components accounted for 5% or more of the CC shape variability in the data set; relationships between their shape component coefficients and blood pressure were analyzed by the regression models. These seven shape components are depicted visually in Figure 3. The shape components indicated that the highest degrees of intersubject variability were present in the splenium (see Figure 3, components A and B) although significant variability was present throughout the structure, including the midbody and genu as well.

Relationship between shape components and blood pressure

Results of linear modeling of relationships between shape component coefficients and systolic blood pressure are reported in Table 2, along with an intuitive description of what each shape component accounts for in terms of CC deficits. Increased atrophy to the more posterior sections of the CC, including the splenium and posterior midbody, was significantly associated with increases in blood pressure, while associations between blood pressure and more anterior CC regions was not significant at the p=.05 level. For the posterior CC shape components, a 1-point increase in blood pressure was associated with a decrease in CC thickness of .16 to .21 mm. Associations between shape component coefficients and diastolic blood pressure are shown in Table 3. As for systolic blood pressure, greater relative atrophy to the posterior midbody was significantly associated

with higher diastolic blood pressure; relationships between greater atrophy to the splenium and higher diastolic blood pressure were not significant but showed a trend towared significance (component A, p=.08; component B, p=.096). Additionally, one shape component covering elongation and thinning of the genu was associated with higher diastolic blood pressure. However, the associations between the two gross-scale CC volumetric measures and systolic and diastolic blood pressure were not statistically significant at the p=.05 level.

Relationship between spatial map and blood pressure

Significance values for correlations between CC radial thickness values and systolic blood pressure are shown in Figure 4. While none of the p values reached statistical significance, they suggest a similar pattern of associations seen with LoCA: the splenium and a portion of the posterior midbody, in particular, have p values that hint a possible association between smaller CC thickness and higher blood pressure. There is an additional, thin strip of genu whose p values hint at an association of this nature.

Discussion

The most consistent finding of this study is that localized measures of increased atrophy in posterior regions of the CC were significantly associated with increases in blood pressure among elderly subjects; these associations did not appear to be driven by a strong relationship between global CC atrophy and blood pressure. A number of studies have found deficits in other brain regions related to hypertension, but we believe this is the first finding of hypertension-related deficits specific to the splenium and posterior midbody. In elderly subjects, any vulnerability of the posterior CC to hypertension effects would complement the apparent susceptibility of the anterior CC to

atrophy associated with increasing age (Weis et al 1993, Parashos et al 1995, Salat et al 1997). Additionally, the posterior CC may be susceptible to atrophy associated with Alzheimer's disease in some elderly subjects (Thompson et al. 1998). While six of the seven atrophy measures significantly associated with blood pressure measures covered the posterior CC, we note that seventh one did cover a portion of the genu. The significance of this finding is unclear.

It is unclear why the posterior CC may be differentially susceptible to atrophic effects of chronic high blood pressure, but we speculate that the relatively vulnerable vascularization of the posterior CC may play a role. The CC receives its blood supply from the anterior communicating artery, the anterior cerebral artery (ACA), and the posterior cerebral artery (PCA; Kasow et al., 2000). In most subjects, the anterior communicating artery branches into the subcallosal and median arteries to supply the genu; the ACA branches into the pericallosal artery to supply the genu and midbody, and the PCA branches into the posterior pericallosal artery to supply the posterior midbody and splenium (Ture et al., 1996). The PCA is generally more tenuous than the other two arteries; for example, while callosal infarction is rare, the PCA is differentially more vulnerable to infarcts than the ACA or anterior communicating artery, and PCA infarction leads to more dramatic callosal atrophy than infarction of the other arteries (Chrysikopoulos et al., 1997). The posterior CC is also more vulnerable to white matter hyperintensities than the anterior CC, suggesting that the PCA may be relatively more susceptible to chronic blood flow dysfunction, or that PCA blood flow dysfunction may have a relatively larger impact on callosal small vessel disease, compared to the ACA or anterior communicating artery (Pekala et al., 2005; Yamamoto et al., 2005). We hypothesize, therefore, that chronic hypertension may have differential effects on the

more posterior CC regions due to the differential vulnerability of the PCA to damage related to chronic blood flow dysfunction.

Additionally, because the CC consists of interhemispheric cortical-cortical axonal tracts, the posterior CC could be differentially vulnerable to hypertension-related atrophy if those tracts are differentially vulnerable to degeneration in hypertension due to neurological events that may be distal to the CC proper. For example, white matter hyperintensities that are strongly tied to cardiovascular risk factors such as hypertension may be prominent in posterior brain regions—especially the temporal and parietal lobes (Yoshita et al., 2006). White matter hyperintensities (WMHs) in interhemispheric temporal-temporal and parietal-parietal tracts could then lead to Wallerian degeneration of the entire tract, and therefore splenium atrophy (Teipel et al., 1998; Meguro et al., 2000; Teipel et al., 2002 and Meguro et al., 2003). Unfortunately, for this study, we lacked anatomically-specific measures of WMH burden in temporal, parietal, and occipital lobes, and therefore could not directly test associations between regional WMH burden and regional CC atrophy. Due to the high prevalence of WMHs in the frontal lobe, we feel that overall WMH burden across the entire brain would be a poor surrogate measure for WMH burden in the more posterior regions, and therefore associating global WMH volume with CC regional atrophy measures would not adequately address this issue.

While the impact of elevated blood pressure on CC morphology is not fully understood, long-term elevated systolic blood pressure is known to exert a chronic negative effect on the integrity of other brain regions (Swan et al., 1998b). Enlarged lateral ventricles, decreased left hemisphere volume, smaller thalamic nuclei volume, and increased temporal lobe cerebrospinal fluid have each been associated with chronic

hypertension (Strassburger et al., 1997, Salerno et al., 1992). Additionally, mid-life blood pressure is associated with late-life hippocampal atrophy, and may contribute to cognitive decline through small-vessel pathology or have a direct link to dementia pathology (Korf et al., 2004; Heijer et al., 2005).

Besides these atrophic effects, hypertension (including borderline hypertension) is recognized as the greatest risk factor for acute brain injury, including stroke (Sacco et al., 1999). Stroke may cause infarction of the CC (Kasow et al., 2000). Also, hypertension is strongly associated with the presence of white matter hyperintensities (WMH) on fluid-attenuated inversion recovery (FLAIR) MRI, which strongly correlate with cognition (Kobayashi et al., 1997; de Leeuw et al., 1999; Yoshita et al., 2006, Dufoil et al., 2001). Several studies have reported that the locations of infarcts and WMH in the CC may follow a specific spatial pattern, suggesting that certain regions of the CC may be more susceptible to acute injury.

Our second key finding is that LoCA, an emerging computational morphology technique, can detect patterns of localized regional atrophy that agree with an established high-dimensional atrophy analysis method. LoCA and the spatial mapping method differ in several significant algorithmic steps—in particular, the spatial mapping method does not do a generalized Procrustes alignment and establishes point-to-point surface correspondences through the use of a medial curve rather than the Ghosh numerical optimization method. Therefore, we did not expect exact agreement in the detected AIDS-control group differences between the two methods. In particular, the superior-anterior CC midbody reflects a localized deficit in the spatial map but not in the shape components, and genu atrophy appears more widespread in LoCA than in the spatial map. However, the degree of congruence between the two methods is high,

providing an encouraging validation for the use of LoCA in this setting. The spatial map of associations between age-corrected systolic blood pressure and local CC thickness in the elderly subjects also agreed with the corresponding LoCA analysis, to the degree that associations between blood pressure and CC atrophy were suggested in the splenium and a portion of the posterior midbody. The *p* values for these associations did not reach statistical significance, however, and a thin strip of genu appeared to show a possible association with systolic blood pressure. We speculate that it may be the ability of LoCA to integrate subtle atrophy measurements over extended local neighborhoods that raised the LoCA results to statistical significance in the splenium, and suppressed spatially isolated, possibly spurious associations in the genu. Each measurement shown on the radial thickness maps, meanwhile, is based on a very isolated, narrow band of the structure; the association between CC thickness and blood pressure may be subtle enough on a point-by-point basis that integration of several measurements over an extended neighborhood may be required to detect it.

The spatial mapping method has previously provided plausible local atrophy measurements in a large number of brain structures and medical conditions, suggesting its viability as a reliable baseline method (see, *e.g.,* Carmichael et al. 2006, Narr et al. 2000, Thompson et al. 2006). The key difference between LoCA and the spatial mapping method is dimensionality: the spatial maps depict hundreds of callosal thickness measurements densely sampled from the callosal surface, while LoCA provides a concise set of roughly ten measurements per CC. Thus, while callosal deficits may be visible in renderings of the spatial maps, the maps are relatively more cumbersome for setting thresholds between normal and abnormal thickness values, or performing statistical analyses. Specifically, in a routine clinical setting, the clinician would need to receive

training in how to visually read the spatial maps and develop a protocol for determining that a spatial map for a particular subject appeared normal or abnormal; as such, the results of applying the spatial maps in practice could vary depending on the computer visualization environment that the maps are viewed in, as well as the training of the clinician. LoCA, on the other hand, provides a small set of numerical measures-- 7 in this case—which can be evaluated succinctly alongside a variety of other relevant clinical measures.

Because the CC is functionally segregated into sub-regions, a number of other methods have been proposed to quantify spatially-localized deficits (Thompson et al., 2001). Geometric partitioning schemes use sets of vertical or radial lines to break a sagittal 2D CC cross-section into sub-regions using predefined rules to determine how the lines should be spaced apart (Witelson et al., 1989, Rajapakse et al., 1996, Stievenart et al., 1997). These schemes can be highly sensitive to the position of the nominal CC landmarks that determine the placement of partitioning lines; for example, the Witelson partition is sensitive to the placement of the most-anterior and most-posterior CC surface point (Clarke et al., 1989, Allen et al., 1991). Image-based CC atrophy methods geometrically align the subject image to a pre-defined digital atlas image and use the properties of the geometric transformation aligning subject CC to atlas CC as a cue for localized CC deficits (Christensen et al., 1994, Davatzikos et al., 1996). The geometric transformations can provide compelling point-to-point correspondences between subject and digital atlas, especially if the transformations are constrained to be biologically plausible (Grenander et al., 1998). However, because the geometric transformations are generally nonlinear, dense, and high-dimensional, relationships between the geometric transformations and variables of interest can be difficult to interpret in intuitive

biological terms without further post-processing of the transformation data. Surface-based CC atrophy methods represent the 2D sagittal CC cross-section of each subject by their delineating contours, and approximate the contours by sets of 2D surface points that are in approximate anatomical correspondence between subjects (Thompson et al., 2006, Alcantara et al 2007). The positions of the surface points, or other statistics derived from the surface point positions, are used as localized measures of CC atrophy. Our method is surface-based and relies on a curvature-based method for sampling points from the subject CC surfaces so that there is approximate anatomical correspondence in point positions between subjects (Ghosh et al 2007).

The key limitation of this study is the relatively small sample of 28 subjects. The sample was selected to allow us to minimize several sources of callosal variability—including age, gender, ethnicity, and presence of neurodegenerative diseases—that could have confounded the effects of hypertension on the CC. However, future work should validate the finding of posterior callosal vulnerability in larger, more diverse elderly subject groups to determine the degree to which hypertension-CC relationships may be modulated by the diverse other factors that are known to impact CC structure in the aging brain.

References

Allen et al. 1991. Sex differences in the corpus callosum of the living human being. The Journal of Neuroscience, 11 (4): 933-942.

Burt el al. 1995. Prevalence of hypertension in the US adult population. Results from the Third National Health and Nutrition Examination Survey, 1988-1991. Hypertension, 25: 305-313.

Carmichael et al 2006. *Mapping Ventricular Changes Related to Dementia and Mild Cognitive Impairment in a Large Community-Based Cohort*. Proceedings, IEEE International Symposium on Biomedical Imaging, April 2006, pp. 315-318.

Christensen et al., 1994. 3D brain mapping using a deformable neuroanatomy. Phys. Med. Biol., 39: 609-618.

Chrysikopoulos et al. 1997. Infarction of the corpus callosum: computed tomography and magnetic resonance imaging. European Journal of Radiology, 25 (1): 2-8.

Clarke et al. 1989. Forms and measures of adult and developing human corpus callosum. Journal of Neuropathology and Experimental Neurology, 280: 213-230.

Davatzikos et al. A computerized approach for morphological analysis of the corpus callosum. J. Comp. Assisted Tomography, 20 (1): 88-97.

DeCarli, Charles. 2004. Vascular factors in dementia: an overview. Journal of the Neurological Sciences, 226: 19-23.

de Leeuw FE, de Groot JC, Oudkerk M, et al. A follow-up study of blood pressure and cerebral white matter lesions. Ann Neurol 1999; 46: 827-833.

Dufouil *et al.* 2001. Longitudinal study of blood pressure and white matter hyperintensities: The EVA MRI Cohort. *Neurology*, 56 (7): 921-926.

Funnell MG, Corballis PM, Gazzaniga MS. 2000. Insights into the functional specificity of the human corpus callosum. Brain, 123 (5): 920-926.

D. Ghosh and N. Amenta, "Landmark transfer using deformable models," Department of Computer Science, University of California, Davis, Tech. Rep. CSE-2007-6, 2007.

Grenander U and Miller M.I. 1998. Computational anatomy: An emerging discipline, Quarterly of Applied Mathematics 56, 617-694.

Gunter LJ et al. 2007. MRI system tracking and corrections using the ADNI phantom. Alzheimer's & Dementia 2007; 3(3):106

Harrington et al. 2000. Cognitive Performance in Hypertensive and Normotensive Older Subjects. Hypertension, 36: 1079-1082.

Harris, TB., et al. Age, Gene/Environment Susceptibility–Reykjavik Study: Multidisciplinary Applied Phenomics. Am J Epidemiol 2007;165:1076–1087.

Heijer et al. *2005*. Association between blood pressure, white matter lesions, and atrophy of the medial temporal lobe. *Neurology*, 64 (2): 263-267.

Janowsky JS, Kaye JA, Carper RA. (1996). Atrophy of the Corpus Callosum in Alzheimer's Disease Versus Healthy Aging. *Journal of the American Geriatrics Society*, 44 (7): 798-803.

Kasow et al. 2000. Corpus Callosum Infarcts with Atypical Clinical and Radiologic Presentations. American Journal of Neuroradiology, 21: 1876-1880.

Kilander et al. 1998. Hypertension is related to cognitive impairment: a 20-year follow-up of 999 men. Hypertension, 31: 780-786.

Kobayashi, S., Okada, K., Koide, H., Bokura, H., & Yamauchi, S. (1997). Subcortical silent brain infarction as a risk factor for clinical stroke. Stroke, 28, 1932-1939.

Korf et al. 2004. Midlife Blood Pressure and the Risk of Hippocampal Atrophy: The Honolulu Asia Aging Study. *Hypertension*, 44 (1): 29-34.

Launer et al. 1995. The association between blood pressure levels and late-life cognitive function: the Honolulu-Asia Aging Study. HAMA, 274: 1846-1851.

Lifton et al., 2001. Molecular mechanisms of human hypertension. Cell, 104 (4) 545-56.

Meguro et al. 2000. Atrophy of the corpus callosum correlates with white matter lesions in patients with cerebral ischaemia. Neuroradiology, 42 (6): 413-419.

Meguro et al. 2003. Corpus Callosum Atrophy, White Matter Lesions, and Frontal Executive Dysfunction in Normal Aging and Alzheimer's Disease. A Community-Based Study: The Tajiri Project. International Psychogeriatrics, 15 (1): 9-25.

Narr KL, Thompson PM, Sharma T, Moussai J, Cannestra AF, Toga AW (2000). *Mapping Corpus Callosum Morphology in Schizophrenia*, Cerebral Cortex, 10(1):40-49, January 2000.

Ong, KL, et al. 2007. Prevalence, Awareness, Treatment, and Control of Hypertension Among United States Adults 1999-2004. Hypertension, 49 (1): 69-75.

IA Parashos, WE Wilkinson and CE Coffey. Magnetic resonance imaging of the corpus callosum: predictors of size in normal adults. J Neuropsychiatry Clin Neurosci 1995; 7:35-41

Pekala JS, Mamourian AC, Wishart HA, Hickey WF, Raque JD (2003) Focal lesion in the splenium of the corpus callosum on FLAIR MR images: a common finding with aging and after brain radiation therapy. Am J Neuroradiol 24:855–861

Rajapakse et al. 1996. Regional MRI measurements of the corpus callosum: a methodological and developmental study. Brain and Development, 18: 379-388.

Sacco RL. 1999. Risk factors and their management for stroke prevention: outlook for 1999 and beyond. Neurology, 53 (7 Supp 4): S15-24.

Salat D, Ward A, Kaye JA, Janowsky JS: Sex differences in the corpus callosum with aging. Neurobiol Aging 1997; 18:191–197

Salerno JA, Murphy DGM, Horwitz B, DeCarli C, Haxby JV, Rapoport SI, Schapiro MB. Brain atrophy in hypertension: a volumetric magnetic resonance imaging study. *Hypertension*. 1992;20:340-348.

Schmidt R, Fazekas F, Koch M, Kapeller P, Augustin M, Offenbacher H, Fazekas G, Lechner H. Magnetic resonance imaging cerebral abnormalities and neuropsychologic test performance in elderly hypertensive subjects: a case controlled study. *Arch Neurol*. 1995;52:905-910.

Skoog et al. 1996. Fifteen-year longitudinal study of blood pressure and dementia. Lancet, 347: 1141-1145.

Skoog, Ingmar; Gustafson, Deborah. 2002. Hypertension and Related Factors in the Etiology of Alzheimer's Disease. Annals of the New York Academy of Sciences, 977: 29-36.

Stievenart et al. 1997. Minimal surface: a useful paradigm to describe the deeper part of the corpus callosum? Brain Res Bull, 44 (2): 117-124.

Strassburger, T., et al. 1997. Interactive Effects of Age and Hypertension on Volumes of Brain Structures. Stroke, 28: 1410-1417.

Swan et al. 1998a. Association of midlife blood pressure to late-life cognitive decline and brain morphology. Neurology, 51 (4): 986-993.

Swan et al. 1998b. Larue Systolic Blood Pressure Tracking Over 25 to 30 Years and Cognitive Performance in Older Adults Stroke, November 1; 29(11): 2334 - 2340.

Teipel et al. 1998. Dissociation between corpus callosum atrophy and white matter pathology in Alzheimer's disease. Neurology, 51, 1381-1385.

Teipel et al. 2002. Progression of Corpus Callosum Atrophy in Alzheimer Disease. Archives of Neurology, 59 (2): 243-248 .

Thompson PM, Moussai J, Khan AA, Zohoori S, Goldkorn A, Mega MS, Small GW, Cummings JL, Toga AW (1998) *Cortical Variability and Asymmetry in Normal Aging and Alzheimer's Disease*, Cerebral Cortex, 8(6):492-509, Sept.1998.

Thompson PM, K. Narr, R. Blanton and A. Toga, Mapping structural alterations of the corpus callosum during brain development and degeneration. In: Marco Iacoboni, Eran Zaidel, Editors, *Proceedings of the NATO ASI on the Corpus Callosum*, Kluwer Academic Press (2001).

Thompson et al. 2006. 3D mapping of ventricular and corpus callosum abnormalities in HIV/AIDS. NeuroImage, 31: 12-23.

Türe et al. 1996. The Arteries of the Corpus Callosum: A Microsurgical Anatomic Study. Neurosurgery, 39 (6): 1075-1085.

Weis, S, Kimbacher, M, Wenger, E, Neuhold, A. Morphometric analysis of the corpus callosum using MR: correlation of measurements with aging in healthy individuals. Am J Neuroradiol 14(3) 1993.

Witelson SF: Hand and sex differences in the isthmus and genu of the human corpus callosum. A postmortem morphological study. Brain 1989;112:799-835.

Woods R.,2001. MultiTracer software package. http: // bishopw.loni.ucla.edu / MultiTracer/ MultiTracer.html

Yamamoto A, Miki Y, Fushimi Y, Okada T, Tomimoto H (2004) Mid-anterior surface of the callosal splenium: subependymal or subpial? Am J Neuroradiol 25:664–665.

Yamamoto et al. 2005. Age-related signal intensity changes in the corpus callosum: assessment with three orthogonal FLAIR images. European Radiology, 15 (11): 2304-2311.

Yoshita et al. 2006. Extent and distribution of white matter hyperintensities in normal aging, MCI, and AD. Neurology, 67: 2192-2198.

Table 1: **Subject characteristics**

Variable	**All Subjects**	**High Blood Pressure Group**	**Normal Blood Pressure Group**	**Group differences (*t*,*p*)**
Age	77.15 +/- 1.57 (75.0,79.0)	77.62 +/- 1.45 (75, 79)	76.4 +/- 1.51 (75,79)	2.04, .06
MMSE	28.15 +/- 1.35 (26,30)	28.0 +/- 1.33 (26, 30)	28.3 +/- 1.42 (26,30)	-.49, .63
Systolic BP	131.6 +/- 23.02 (99,170)	144.4 +/- 20.25 (99, 170)	111.2 +/- 6.0 (102,119)	**6.14, 6.9e-6**
Diastolic BP	70.65 +/- 7.36 (57,82)	72.7 +/- 8.10 (57, 82)	67.4 +/- 4.72 (60,76)	**2.10, .046**
9-Slice CC Volume	5469 +/- 648.3 mm^3 (4241,6805)	5498 +/- 624.83 (4241, 6600)	5421 +/- 716.06 (4317,6805)	.28, .783

Summary variables for subjects in this study. All subjects were right-handed Icelandic females between 75 and 79 years of age with MMSE>=26, no evidence of clinical depression, and no consensus diagnosis of cognitive impairment. Each quantity is reported as Mean +/- Standard Deviation (Min, Max). Results of *t* tests between normal blood pressure and high blood pressure groups are shown. Tests with $p<.05$ are shown in bold.

Table 2

Table 2: Relationship between systolic blood pressure and localized measures of callosal atrophy, controlling for subject age.

Shape Component	Description	Regression Parameter (mm/BP)	F	p
A	**Thinner splenium**	**0.186**	**4.849**	**0.038**
B	**Thinner splenium relative to posterior midbody**	**0.190**	**5.615**	**0.027**
C	Thinner and more elongated genu	0.104	1.368	0.254
D	**Thinner inferior-posterior midbody**	**0.215**	**5.698**	**0.026**
E	Thinner and more curved genu	0.026	0.077	0.784
F	Thinner inferior-anterior midbody	0.095	1.517	0.230
G	**Thinner posterior midbody relative to central midbody**	**0.160**	**6.269**	**0.020**
Overall CC volume		2.32 (mm^3/year)	0.112	0.741
Overall CC size (GPA scaling parameter)		-6.97e-06	0.190	0.667

The relationship between systolic blood pressure and global morphometric measures -- overall volume, and overall size from GPA scaling-- is also shown.

Table 3

Table 2: Relationship between diastolic blood pressure and localized measures of callosal atrophy, controlling for subject age.

Shape Component	Description	Regression Parameter (mm/BP)	F	p
A	Thinner splenium	0.443	3.300	0.082
B	Thinner splenium relative to posterior midbody	0.408	3.010	0.096
C	**Thinner and more elongated genu**	**0.515**	**4.840**	**0.038**
D	**Thinner inferior-posterior midbody**	**0.669**	**7.484**	**0.012**
E	Thinner and more curved genu	0.179	0.469	0.500
F	Thinner inferior-anterior midbody	0.242	1.241	0.277
G	**Thinner posterior midbody relative to central midbody**	**0.510**	**8.798**	**0.0069**
Overall CC volume		10.50 (mm^3/year)	0.293	0.594
Overall CC size (GPA scaling parameter)		-9.20e-07	0.638	0.432

The relationship between diastolic blood pressure and global morphometric measures -- overall volume, and overall size from GPA scaling-- is also shown.

Figure 1
Click here to download 5. Figure: Figure1.pdf

Figure 1: Top: CC spatial map from (Thompson et al., 2006) with significant differences between HIV/AIDS and control groups in localized CC thickness shown in red. Bottom: LoCA shape components whose coefficients were significantly different between AIDS and controls are shown in green (two-tailed *t* tests). Qualitatively, there is high agreement between significantly different regions according to the spatial map (shown in red in the top figure) and the significantly different regions according to LoCA (shown with blue arrows in the green-background sub-figures below). Specifically, both methods indicate significant genu and anterior midbody atrophy. We note, however that there are minor discrepancies between the two: atrophy to the superior-anterior midbody was detected by the spatial map but not LoCA; and genu atrophy is relatively more extensive in LoCA.

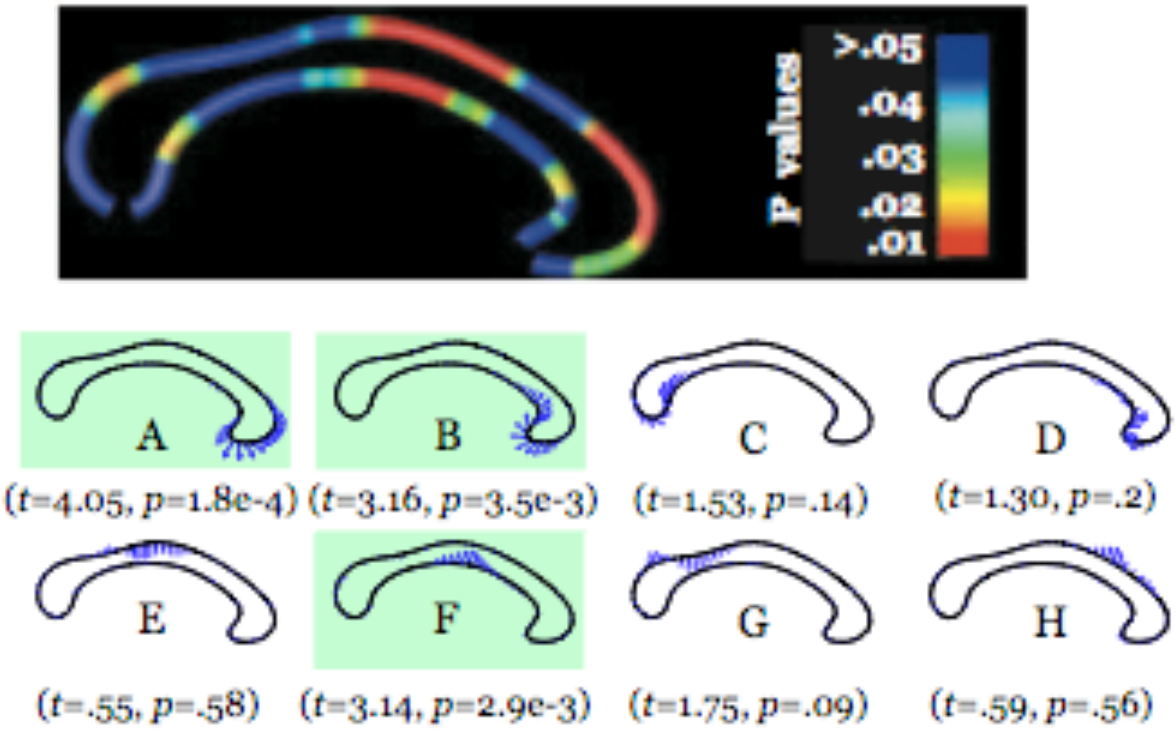

Figure 2
Click here to download 5. Figure: Figure2.pdf

Figure 2: Power spectrum of shape components.

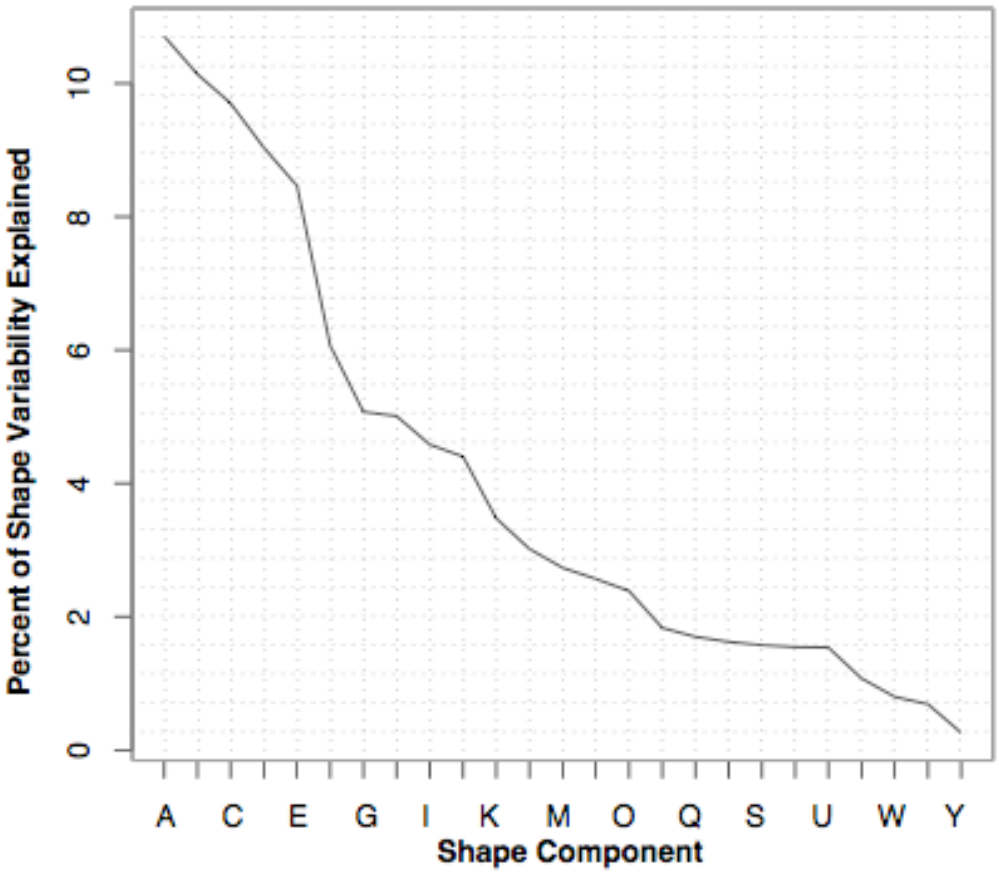

Figure 3
Click here to download 5. Figure: Figure3.pdf

Figure 3: Graphical depiction of the callosal shape components analyzed in regression models.

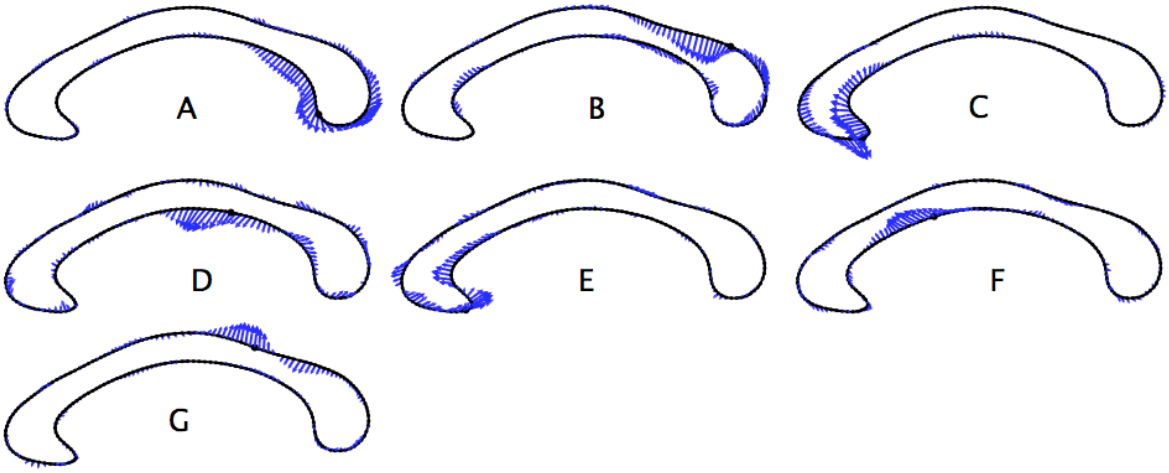

download 5. Figure: Figure4.pdf

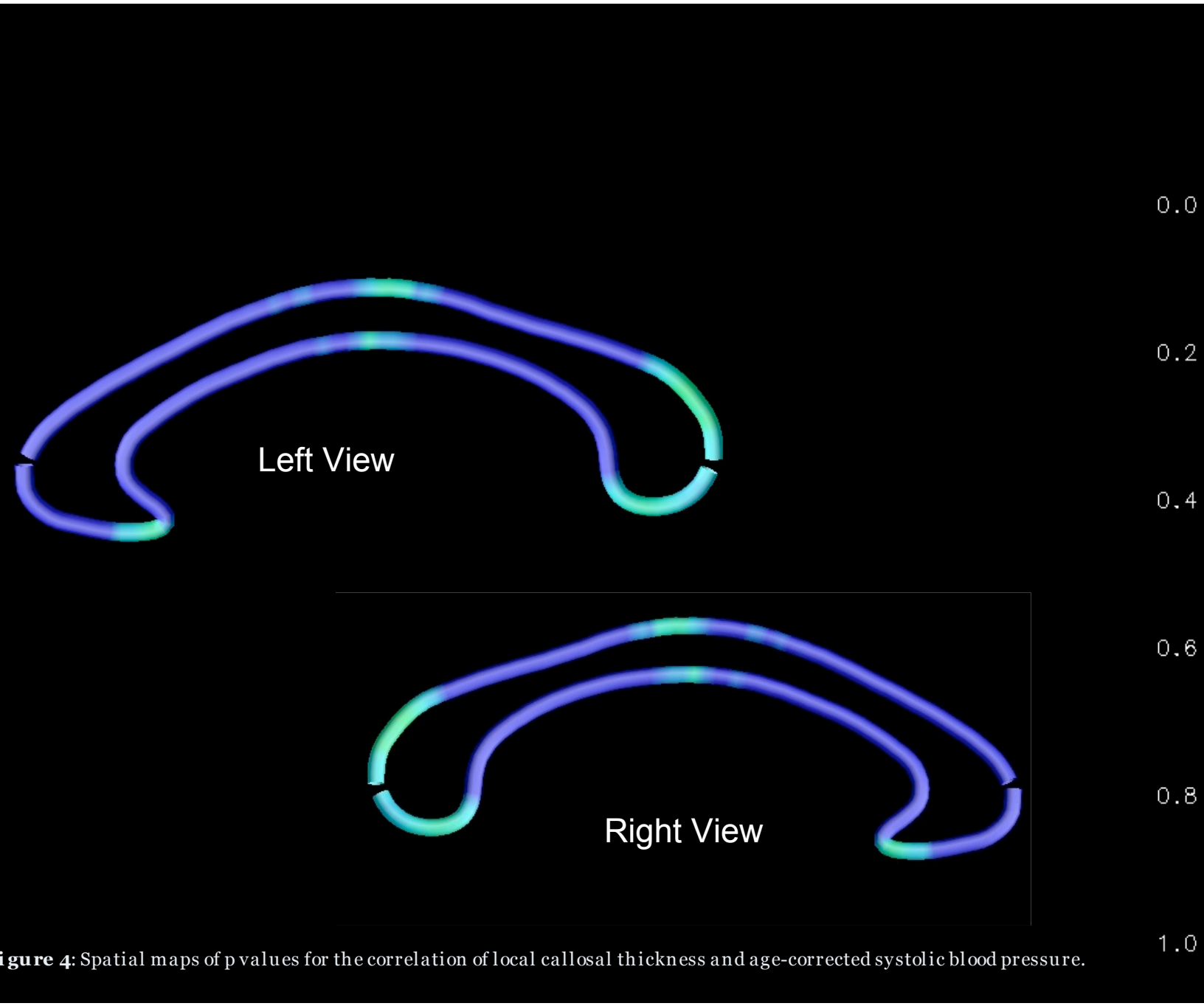

igure 4: Spatial maps of p values for the correlation of local callosal thickness and age-corrected systolic blood pressure.